EDGE ARTICLE

Check for updates

Modulating luminescence and assembled shapes of ultrasmall Au nanoparticles towards hierarchical information encryption†

Tingyao Zhou and Xingyu Jiang [ID] *

Because of their intriguing luminescence performances, ultrasmall Au nanoparticles (AuNPs) and their assemblies hold great potential in diverse applications, including information security. However, modulating luminescence and assembled shapes of ultrasmall AuNPs to achieve a high-security level of stored information is an enduring and significant challenge. Herein, we report a facile strategy using Pluronic F127 as an adaptive template for preparing Au nanoassemblies (AuNAs) with controllable structures and tunable luminescence to realize hierarchical information encryption through modulating excitation light. The template guided ultrasmall AuNP *in situ* growth in the inner core and assembled these ultrasmall AuNPs into intriguing necklace-like or spherical nanoarchitectures. By regulating the type of ligand and reductant, their emission was also tunable, ranging from green to the second near-infrared (NIR-II) region. The excitation-dependent emission could be shifted from red to NIR-II, and this significant shift was considerably distinct from the small range variation of conventional nanomaterials in the visible region. In virtue of tunable luminescence and controllable structures, we expanded their potential utility to hierarchical information encryption, and the true information could be decrypted in a two-step sequential manner by regulating excitation light. These findings provided a novel pathway for creating uniform nanomaterials with desired functions for potential applications in information security.

Introduction

Optical multiplexing presents an attractive prospect for exploring potential applications in chemical sensors, bioimaging, information storage and encryption.[1–3] Advanced multiplexing for information encryption requires novel luminescent materials with well-defined nanostructures, unique physicochemical properties and excellent stability.[4,5] Various strategies have been developed to regulate the luminescence behaviours of luminescence materials by changing external stimuli, such as excitation light, heat stimuli, chemical reagents, and mechanical stimuli, to ensure high-level information security.[6–8] Among these strategies, regulation of excitation light is appealing due to its low cost, simple operation, non-invasive control and easy detection.[9,10] In the past few decades, a broad range of luminescent nanomaterials, including lanthanide-doped nanoparticles,[11–15] perovskite nanocrystals,[16] and semiconducting quantum dots (QDs),[17] have been rationally designed and adopted for information storage and encryption applications based on the regulation of excitation light. However, these nanomaterials usually suffer from poor stability in humid environments, high toxicity from hazardous ions, or high precision control of multiple dopant ions and complicated multistep growth. Thus, it is highly desirable to explore alternative luminescent nanomaterials to promote hierarchical information protection.

Due to their molecule-like properties, low toxicity, superior photo-stability and ease of preparation, ultrasmall gold nanoparticles (AuNPs) are an emerging class of luminescent nanomaterials,[18–21] and their intriguing photoluminescence enables them to be promising for use in sensing, electronics, nanomedicine, information storage and anti-counterfeiting.[22–27] Luminescence tunability is critical to achieving multiplexed coding and hierarchical information encryption. Generally, the luminescence performance of ultrasmall AuNPs can be tuned by ligand engineering, metallic kernel alloying and variation of external environmental factors to gain different emissions from blue to red.[28] Recently, the emission of ultrasmall AuNPs has been expanded to a second near-infrared (NIR-II) region using strong reductant $NaBH_4$.[29–31] Amphiphilic block copolymer-assisted self-assembly provides an effective path for the construction of hierarchical nanoarchitectures and offers an opportunity to explore collective properties.[32] In this approach, amphiphilic block copolymers could be rationally designed by manipulating the block segments and assembled to build

Shenzhen Key Laboratory of Smart Healthcare Engineering, Department of Biomedical Engineering, Southern University of Science and Technology, 1088 Xueyuan Road, Nanshan District, Shenzhen, Guangdong 518055, P. R. China. E-mail: jiang@sustech.edu.cn

uniform micelles with controllable size and shape, which could be used as nanoreactors for the growth and assembly of NPs.[33,34] Besides, the optical features of the building blocks, ultrasmall Au NPs, could be easily *in situ* tuned by controlling experimental conditions, including the concentration of the precursors, type of stabilizers and reducing agents to reach the multicolor emissions and enhancement of luminescence and stability.[35,36] The distinct assembled structures with tunable emission and controllable morphology may provide a new route to make stored information more secure and robust due to difficulties in imitating and enhanced stability. Nevertheless, it is hard to achieve the facile *in situ* construction of luminescent AuNP-based assemblies with simultaneous regulation of morphology and emission, and the application of ultrasmall AuNP-based assemblies in hierarchical information encryption is still not explored adequately.

Hence, a facile and robust approach was reported to *in situ* prepare different types of water-soluble Au nanoassemblies (AuNAs) with controllable structures and tunable luminescence for information storage and hierarchical encryption using Pluronic F127 as a template (Scheme 1). This approach was convenient, cost-efficient, easy to repeat, and environmentally friendly. Pluronic F127, a typical linear amphiphilic block copolymer, could form structurally variable micelles by weak interactions, offering an adaptive template for preparing uniform AuNAs with distinct structures.[37,38] The ultrasmall AuNPs were *in situ* produced in the inner core of the template and organized into distinct nanostructures with necklace-like or spherical shapes in a controllable manner. Their emission was also tunable ranging from green to the NIR-II region by regulating the thiol ligand and reductant type. The necklace-like AuNAs were also controllable for encapsulated NP numbers and greatly distinct from previous reports based on self-assembly of pre-prepared AuNPs,[39,40] which usually underwent rigorous assembly conditions, low efficiency and luminescence quenching during self-assembly. More importantly, we obtained a kind of intriguing Au NA with excitation light-dependent emission, which could emit a strong red light identical to that emitted by another Au NA under UV light at 300 nm and could give an outstanding NIR-II emission excited by an 808 nm laser. Additionally, the obtained AuNAs were remarkably stable in their emission and assembled structures to ensure long-term information storage. It was more difficult to imitate for information storage and encryption due to the same Au-related materials and intrinsically assembled nano-structures. Utilizing their unique features, we used these AuNAs as primitives for coding information and modulated the excitation light to achieve hierarchical information encryption and decryption, largely expanding their potential utility to multiple information encryption.

Results and discussion

Using Pluronic F127 as a typical template, four different AuNAs composed of ultrasmall AuNPs were synthesized with a one-pot protocol in the presence of the hydrophobic thiolate ligands and reducing agent tetrakis (hydroxymethyl) phosphonium chloride (THPC, Scheme 1a). Four kinds of hydrophobic bidentate thiol ligands with similar structures, including 1,3-propanedithiol (3CS$_2$), 1,4-butanedithiol (4CS$_2$), 1,8-octanedithiol (8CS$_2$), and ethylene bis(3-mercaptopropionate) (10CS$_2$), were employed for the preparation of AuNAs, and the obtained AuNAs were denoted as 3CS$_2$ AuNAs, 4CS$_2$ AuNAs, 8CS$_2$ AuNAs and 10CS$_2$ AuNAs, respectively. As shown in Fig. 1a, the four
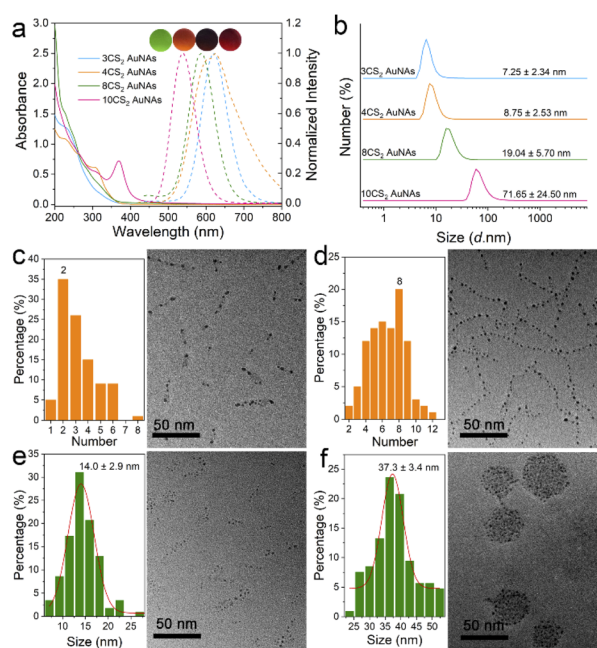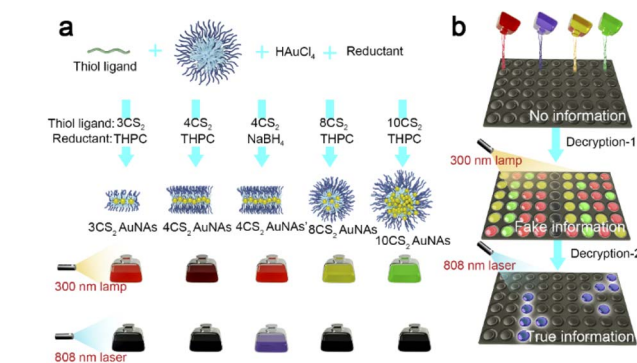

Fig. 1 Synthesis and characterization of the AuNAs. (a) UV–vis absorption and luminescence spectra of the AuNAs using 3CS$_2$, 4CS$_2$, 8CS$_2$ and 10CS$_2$. The inset (from left) shows photographs of the solution of the 10CS$_2$ AuNAs, 8CS$_2$ AuNAs, 4CS$_2$ AuNAs and 3CS$_2$ AuNAs under UV illumination at 300 nm. (b) HDs of the four types of the AuNAs. TEM image of the 3CS$_2$ AuNAs (c) and 4CS$_2$ AuNAs (d), and the probability distribution of encapsulated AuNP numbers in an assembly obtained from TEM images. TEM image of the 8CS$_2$ AuNAs (e) and 10CS$_2$ AuNAs (f), and size distribution of the assembled structures obtained from TEM images.

Scheme 1 Schematic illustration of the *in situ* synthesis process for AuNAs and hierarchical encryption. (a) The typical synthesis process for AuNAs by regulating the type of ligand and reductant. (b) Scheme of hierarchical encryption by modulating excitation light.

types of AuNAs showed distinct absorbance characteristics in the 200–400 nm region. No surface plasmonic resonance absorbance appeared at 520 nm, indicating the existence of the AuNAs with different structures and no formation of large plasmonic AuNPs during the *in situ* fabrication. Under UV illumination at 300 nm, the AuNA solution using $3CS_2$, $4CS_2$, $8CS_2$, and $10CS_2$ emitted red, deep red, orange, and green light with an emission peak at 620, 608, 587 and 537 nm, respectively, illustrating that the AuNAs displayed luminescence tunability and multicolor emissions. The blue-shifted emission could probably be attributed to the ratio of Au(I) to Au (0) species enhancement with increasing the carbon chain skeleton length of thiol ligands (Fig. S1†).[41] The corresponding hydrodynamic diameter (HD) was also found to be different and increased from 7.25 to 71.65 nm with increasing the carbon chain skeleton length of thiol ligands (Fig. 1b), indicating the structural difference of the AuNAs. Transmission electron microscopy (TEM) images demonstrated that the $3CS_2$ AuNAs and the $4CS_2$ AuNAs were composed of approximately 2 and 8 ultrasmall AuNPs, and these ultrasmall AuNPs were organized into an intriguing necklace-like shape (Fig. 1c, d and S2†). In contrast, spherical assembled nanostructures were observed for the AuNAs using $8CS_2$ and $10CS_2$ with assembling sizes of 14.0 ± 2.9 nm and 37.3 ± 3.4 nm (Fig. 1e and f). Besides, we observed that as the carbon chain skeleton of bidentate thiol ligands became longer, the core size of ultrasmall AuNPs gradually diminished from 2.9 ± 0.5 nm for the $3CS_2$ AuNAs to 1.5 ± 0.3 nm for the $10CS_2$ AuNAs (Fig. S3†). These four types of AuNAs were remarkably stable, as their emission intensity did not decrease and no obvious change in their assembled structures occurred even after being stored for 4 months (Fig. S4 and S5†). The above results pointed out that AuNAs with controllable morphology and excellent luminescence could be achieved, further revealing this block copolymer-assisted self-assembly's high controllability and luminescence tunability.

It was intriguing to one-pot synthesize the necklace-like AuNAs in a controllable manner, which was largely different from the self-assembly of the pre-prepared NP strategy.[39,40] The one-pot protocol was simple and convenient, effectively avoiding the aggregate generation during self-assembly of pre-prepared NPs. Thus, it was interesting to explore the mechanism for one-pot synthesis of the necklace-like AuNAs. In a typical synthesis of necklace-like $4CS_2$ AuNAs, Pluronic F127 could self-assemble to form uniform hydrophobic core-hydrophilic shell micelles,[42,43] which could be used as the template. Due to the hydrophobic interaction of $4CS_2$ ligands and strong Au-thiol coordination, ultrasmall AuNPs were favorable to be produced and self-assembled in a hydrophobic core. In this synthetic process, the template Pluronic F127 retained a spherical structure, as its HD maintained at about 20 nm until the dialysis process (Fig. S6†), indicating that the original AuNAs were supposed to consist of several ultrasmall AuNPs in the hydrophobic core and be surrounded by a hydrophilic PEO shell on their surface. After dialysis against water, the HD of the template reduced to 8.7 nm (Fig. 1b), suggesting that the template produced a change in the structure and might guide ultrasmall AuNP redistribution to minimize the system

energy. From the X-ray photoelectron spectroscopy (XPS) results (Fig. 2a and b), it was found that the peak intensity at 286.3 eV (C–O bonds) decreased, and the apparent enhancements for C–C bonds at 284.8 eV and Au signals occurred after Ar$^+$ sputtering treatment,[44] illustrating that the AuNPs were mainly located in the hydrophobic inner core of the template and were surrounded by a PEG layer on their surface. Atomic force microscopy (AFM) was a preferred technique for directly measuring polymers.[45] The AFM image also showed that the $4CS_2$ AuNAs presented defined linear nanostructures with a width size of 6.3 ± 1.8 nm, which was larger than the size of ultrasmall AuNPs because of measurement by AFM including the surface PEG layer from the template (Fig. 2c and S7†), convincingly confirming that the deformed template Pluronic F127 provided a powerful scaffold for directing ultrasmall AuNPs in confined spaces into necklace-like nanostructures. To gain a deep insight into the chemical information of the $4CS_2$ AuNAs, we employed high-angle annular dark-field (HAADF) scanning transmission electron microscopy (STEM) and elemental mapping (Fig. 2d and S8†). The HAADF-STEM image showed that $4CS_2$ AuNAs had an amazing necklace-like morphology. The elemental mapping illustrated that the hydrophobic thiol ligands $4CS_2$ mainly distributed around the ultrasmall AuNPs. The interaction between ultrasmall AuNPs
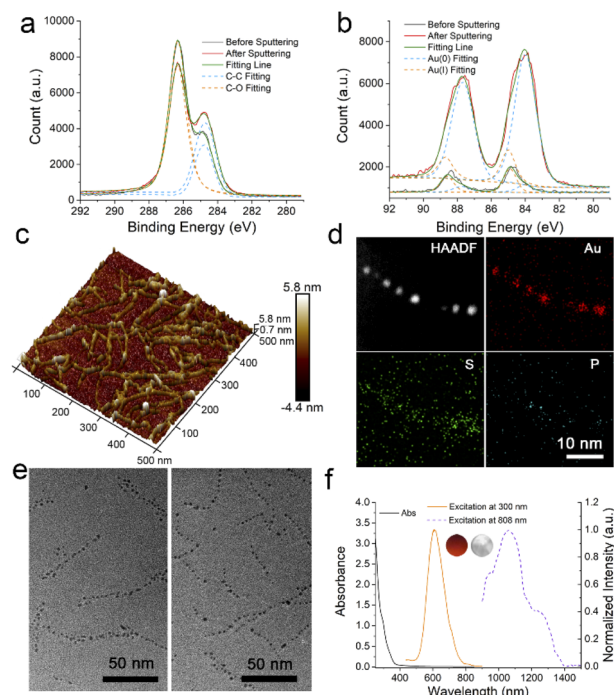

Fig. 2 The assembling mechanism for the necklace-like AuNAs. C1s (a) and Au4f (b) XPS spectra of the $4CS_2$ AuNAs before and after Ar$^+$ sputtering. (c) AFM image of the $4CS_2$ AuNAs. (d) HAADF-STEM image and the elemental mapping for the $4CS_2$ AuNAs. (e) TEM image of the AuNAs using template F108 (left) and the $4CS_2$ AuNAs' prepared with NaBH$_4$ (right). (f) The UV-vis absorption and emission spectra of the $4CS_2$ AuNAs', and the inset (from left) showed photographs of the solution of $4CS_2$ AuNAs under UV illumination at 300 nm and under 808 nm laser irradiation.

and phosphorus ligands from the reducer THPC was not obvious because of the weak P signal, indicating that ultrasmall AuNPs were protected by hydrophobic thiol ligands $4CS_2$ and located in the hydrophobic inner core of the template. The above results unambiguously demonstrated that the one-pot synthesis of 1D necklace-like AuNAs with controllable dimensions was achieved by assistance of structurally alterable template Pluronic F127.

To further explore the mechanism for the one-pot synthesis of the 1D necklace-like AuNAs, the role of thiol ligands was studied. The AuNAs using $3CS_2$ presented similar necklace-like nanostructures to the $4CS_2$ AuNAs but only composed of about 3 ultrasmall AuNPs (Fig. 1c). As the carbon chain skeleton of bidentate thiol ligands extended longer than pentane, the AuNAs tended to be spherical as follows: the necklace-like and spherical shape coexisted for the AuNAs using 1,5-pentanedithiol ($5CS_2$), 1,6-hexanedithiol ($6CS_2$), and 1,7-heptanedithiol ($7CS_2$), and the spherical ratio increased from 30% and 42%, to 82% using $5CS_2$, $6CS_2$ and $7CS_2$. In contrast, only spherical nanostructures were observed for the AuNAs using $8CS_2$ and $10CS_2$ (Fig. 1e, f, and S9–S11†). It was because bidentate thiol ligands with longer carbon chain skeletons could establish a strong bridge connection among these ultrasmall AuNPs in the hydrophobic inner core and enhance the structural stability of assemblies against dialysis dilution. In contrast, the shorter bidentate thiol ligands such as $4CS_2$ produced weaker bridge connections. They were insufficient to hold the assembly's original morphology against dialysis dilution, causing the template to deform into a chain-like shape and guiding ultrasmall AuNPs to assemble into the necklace-like nanostructures. We also studied the preparation of Au NPs without bidentate thiol ligands. The surface plasmonic resonance absorbance appeared at around 520 nm (Fig. S12†), revealing that large AuNPs were generated without protection from bidentate thiol ligands. The TEM image also presented the existence of large AuNPs (Fig. S13†). To further reveal the role of bidentate thiol ligands, we investigated the structure and luminescence of AuNAs prepared with different concentrations of $4CS_2$ ligands. As the concentrations of $4CS_2$ ligands changed, their assembled shape remained necklace-like (Fig. S13†), and the emission spectrum, including spectral shape and peak, also stayed the same except for the emission intensity (Fig. S14†). Besides, no apparent change of $4CS_2$ AuNAs in the emission peak and shape was observed when assembled structures changed from spherical to necklace-like through dialysis against water (Fig. S15†). These results further demonstrated that bidentate thiol ligands played an essential role in the assembled shape and emission peak.

As expected, the template Pluronic F127 played a significant role in the one-pot synthesis of the nanonecklaces. The reaction without template Pluronic F127 was conducted in the tetrahydrofuran phase as a control, and the product was a random aggregate containing ultrasmall AuNPs without a necklace-like structure (Fig. S16†). Pluronic F108 and P123, very common kinds of triblock copolymers, were also used as the synthesis templates, respectively. Pluronic F108 with a high weight fraction of the hydrophilic block, which could usually be assembled

into spherical micelles, produced analogical nanonecklaces to F127 due to the structural deformation behaviour (Fig. 2e). In contrast, P123 with a lower weight fraction of the hydrophilic block usually formed lamellar micelles without a flexible structure,[46] giving lamellar-like AuNP-based nanoarchitectures (Fig. S17†), revealing that the rational selection of block polymers with an adaptable weight fraction of the hydrophilic block was crucial to the formation of the necklace-like nanostructures.

As a comparative study for the reductant THPC, $NaBH_4$, a stronger reducing agent than THPC, was used in the fabrication process. The obtained AuNAs using $NaBH_4$ denoted as $4CS_2$ AuNAs', also presented a similar necklace-like shape with a AuNP size of 2.2 ± 0.5 nm to the $4CS_2$ AuNAs (Fig. 2e). More importantly, they not only could emit a strong red light identical to that emitted by $3CS_2$ AuNAs under UV light at 300 nm, which could not be distinguished from each other by the naked eye, but they could give an outstanding NIR-II emission excited by an 808 nm laser (Fig. 2f). According to recent research, the red and NIR-II emissions arose from the core–shell charge transfer state and the NP core state, respectively.[47] Being similar to those of $4CS_2$ AuNAs, XPS spectra of $4CS_2$ AuNAs' (Fig. S18†) showed a decrease of a dominant peak associated with C–O bonds (286.3 eV), and the peak assigned to C–C bonds (284.8 eV) became evident along with the considerable enhancement of Au signals after Ar^+ sputtering treatment. The ratio of Au(I) to Au(0) species was 0.096 due to the strong reducibility of $NaBH_4$. These results suggested that the $4CS_2$ AuNAs' presented a unique core–shell structure capped by a hydrophilic PEG layer on the surface. With an increase in the amount of $NaBH_4$, the emission intensity at 610 nm gradually decreased, while the emission intensity at 1055 nm gradually enhanced (Fig. S19†), implying that the luminescence features could be tunable by the modulation of the reducing agent besides altering the types of bidentate thiol ligands.[48] We also synthesized the AuNAs using $5CS_2$ as the ligand and $NaBH_4$ as the reductant. The TEM image showed that the necklace-like and spherical shapes coexisted (Fig. S20†), indicating that reductants had no significant impact on their assembled shapes. The assembled morphologies mainly depended on the choice of bidentate thiol ligands with different lengths of carbon chains and triblock copolymer templates.

The luminescence tunability and structural controllability of the AuNAs offered a novel type of luminescent nanomaterial suitable for hierarchical information encryption. Different from individual ultrasmall AuNPs, these unique assembled nanostructures were significant for information security and anti-counterfeiting due to more difficulties in imitating. As a proof of concept, we utilized $3CS_2$ AuNAs (red spots) and $4CS_2$ AuNAs' (purple spots) as the primitives for coding the information pattern and the decryption procedure was carried out in a stepwise manner by modulating excitation light (Fig. 3a and b). Under 300 nm UV irradiation, the patterned dots were encrypted first. They presented an identical red emission, making fake information of the "88" symbol due to the undistinguishable luminescence exposed by the UV light. However, the true information of the "20" symbol could be decrypted in
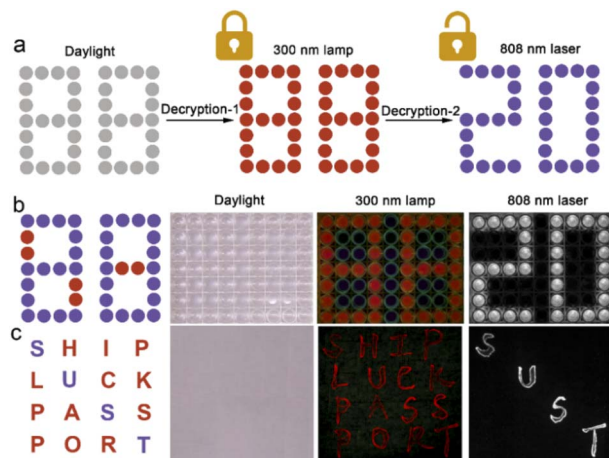
Fig. 3 Information storage and hierarchical encryption of the AuNAs. (a) Schematic diagram of the hierarchical encryption and decryption processes. Photographs of the information pattern on a chip (b) and a square letter array written on a filter paper (c) under daylight, 300 nm lamp radiation and 808 nm laser radiation.
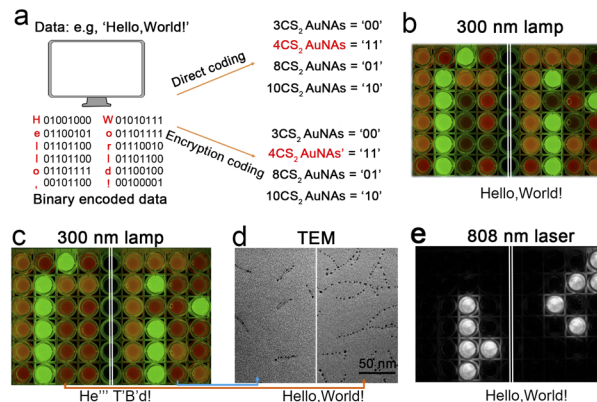

Fig. 4 The utility of these AuNAs in multiplexing recording and hierarchical encryption. (a) Schematic illustration of coding text information with the AuNAs in two different ways: direct coding and encryption coding. (b) The four-color array pattern under 300 nm lamp irradiation. (c) The array pattern involved misinformation under 300 nm lamp irradiation. (d) Typical TEM images from similar color emitting pattern dots. (e) The array pattern under 808 laser irradiation.

a second step by the regulation of excitation light to 808 nm. To further illustrate the performance in hierarchical information encryption, the letters SUST were encrypted within a square letter array and handwritten on a piece of filter paper (Fig. 3c). The four letters "SUST" were written using $4CS_2$ AuNAs', while the other letters were written using $3CS_2$ AuNAs. The letter array was nearly invisible in daylight. Upon irradiation with UV light, the information was encrypted in a first step, and the letter array became visible, but the letters "SUST" were still hidden in them. Once the excitation light changed to an 808 nm laser, the encrypted information "SUST" appeared in a second step due to the unique NIR-II emission of $4CS_2$ AuNAs'.

Taking advantage of their tunable luminescence and diverse structure, we further explored the potential utility of these AuNAs in multiplexing recording and hierarchical encryption. For example, these AuNAs with different shapes and emissions were employed to code text information of "Hello,World!" according to the binary codes of the standard 8 bit ASCII characters, and the decryption was performed in a stepwise manner by sequentially modulating excitation light of 300 nm to 808 nm (Fig. 4a and Scheme 1b). As a control, the text information was straight encoded using these AuNAs, where $3CS_2$ AuNAs = 00, $4CS_2$ AuNAs = 11, $8CS_2$ AuNAs = 01, and $10CS_2$ AuNAs = 10. Under 300 nm UV radiation, a four-color array pattern was observed, and the included information could be accurately decoded into the raw information of "Hello,World!" according to the ASCII binary codes (Fig. 4b). To further strengthen this complex information encryption, $4CS_2$ AuNAs' were used as primitive data 11 instead of $4CS_2$ AuNAs during the coding process. A color-emitting array pattern appeared when exposed to the UV light as decryption-1 (Fig. 4c), producing fake information of "He'''T'B'd!" due to the undistinguishable emission between $4CS_2$ AuNAs' and $3CS_2$ AuNAs under this condition.[49] To obtain the right message, a TEM reader and an 808 nm laser were next employed as decryption-2.

As shown in Fig. 4d, typical TEM images presented an obvious difference in the assembled structures between two similar emitting-color pattern dots. The short nanonecklaces containing about 3 ultrasmall AuNPs were assigned to $3CS_2$ AuNAs. In contrast, the long nanonecklaces containing about 8 ultrasmall AuNPs were assigned to $4CS_2$ AuNAs', illustrating that the hidden information could be deciphered and translated into the right text through identification of different assembled structures. Furthermore, by regulation of excitation light to 808 nm, the pattern dots assigned to $4CS_2$ AuNAs' could be accurately identified, deciphering the true information "Hello,World!" by combining with the color-emitting array pattern under UV light (Fig. 4e). It should be noted that the multicolor emissions arose from the same Au-related materials, and different emitting AuNAs presented distinct assembled structures. Even if the elementary composition was deciphered by inductively coupled plasma mass spectrometry (ICP-MS), it would be more difficult to imitate, which is significant for information security and anti-counterfeiting. These observations confirmed that the AuNAs with luminescence tunability and structural controllability could be used as primitives for coding information and had great potential for hierarchical information encryption.

Conclusions

In conclusion, we presented a robust strategy for *in situ* synthesis of well-defined AuNAs in a controllable and tunable manner by amphiphilic block copolymer-assisted self-assembly. The amphiphilic block copolymer template not only guided ultrasmall AuNPs to *in situ* production in the inner core and organizing them into well-ordered nanostructures but also enabled the obtained AuNAs to have unique core–shell structures capped by hydrophilic PEG chains on the surface. The assembled morphologies were controllable from neck-like to

spherical shapes by regulating the bidentate thiol ligands with different lengths of carbon chains. The rational selection of amphiphilic templates was also crucial to forming the necklace-like nanostructures. Their emission was also tunable by regulating the type of ligand and reductant. More interestingly, we obtained a kind of Au NA with excitation light-dependent emission, which could emit a strong red light and NIR-II emission under a 300 nm lamp and an 808 nm laser, respectively. In virtue of their tunable luminescence and controllable structure, we applied them to information storage and hierarchical encryption. The true information could be decrypted stepwise by regulation of excitation light. These findings not only provided a new method for creating ultrasmall AuNP-based necklace-like nanostructures in a controllable manner but also offered a new encoding concept for information security. In the future, we are convinced that the *in situ* synthesis of well-defined AuNAs in combination with microfluidics may offer new horizons in generating functional nanomaterials with more precise control and higher reproducibility, and the introduction of new technologies such as inkjet printing and fluorescence microscopy would further improve the storage capacity for next-generation information security.

Data availability

All experimental supporting data are available in the ESI.†

Author contributions

T. Z. and X. J. conceived the study; T. Z. performed the experiments; T. Z. and X. J. wrote and revised the manuscript.

Conflicts of interest

There are no conflicts to declare.

Acknowledgements

Notes and references

1 Y. Lu, J. Zhao, R. Zhang, Y. Liu, D. Liu, E. M. Goldys, X. Yang, P. Xi, A. Sunna, J. Lu, Y. Shi, R. C. Leif, Y. Huo, J. Shen, J. A. Piper, J. P. Robinson and D. Jin, *Nat. Photonics*, 2014, **8**, 32–36.

2 J. Xu, J. Zhou, Y. Chen, P. Yang and J. Lin, *Coord. Chem. Rev.*, 2020, **415**, 213328.

3 X. Liu, Y. Wang, X. Li, Z. Yi, R. Deng, L. Liang, X. Xie, D. T. B. Loong, S. Song, D. Fan, A. H. All, H. Zhang, L. Huang and X. Liu, *Nat. Commun.*, 2017, **8**, 899.

4 B. L. Ma, X. Zhai, G. Du and J. Zhou, *Chem. Sci.*, 2019, **10**, 3281–3288.

5 Y. Ou, W. Zhou, Z. Zhu, F. Ma, R. Zhou, F. Su, L. Zheng, L. Ma and H. Liang, *Angew. Chem., Int. Ed.*, 2020, **59**, 23810–23816.

6 K. Jiang, Y. Wang, C. Cai and H. Lin, *Adv. Mater.*, 2018, **30**, e1800783.

7 S. Xu, W. Wang, H. Li, J. Zhang, R. Chen, S. Wang, C. Zheng, G. Xing, C. Song and W. Huang, *Nat. Commun.*, 2020, **11**, 4802.

8 H. Suo, Q. Zhu, X. Zhang, B. Chen, J. Chen and F. Wang, *Mater. Today Phys.*, 2021, **21**, 100520.

9 X. W. Yu, H. Y. Zhang and J. H. Yu, *Aggregate*, 2021, **2**, 20–34.

10 S. Liu, X. Liu, J. Yuan and J. Bao, *Research*, 2021, **2021**, 7897849.

11 J. C. Zhang, C. Pan, Y. F. Zhu, L. Z. Zhao, H. W. He, X. Liu and J. Qiu, *Adv. Mater.*, 2018, **30**, e1804644.

12 P. Verma, A. Singh and T. K. Maji, *Chem. Sci.*, 2021, **12**, 2674–2682.

13 J. Zuo, Q. Li, B. Xue, C. Li, Y. Chang, Y. Zhang, X. Liu, L. Tu, H. Zhang and X. Kong, *Nanoscale*, 2017, **9**, 7941–7946.

14 Y. Han, C. Gao, Y. Wang, D. Ju, A. Zhou, F. Song, L. Huang and W. Huang, *Phys. Chem. Chem. Phys.*, 2018, **20**, 9516–9522.

15 H. Tan, G. Gong, S. Xie, Y. Song, C. Zhang, N. Li, D. Zhang, L. Xu, J. Xu and J. Zheng, *Langmuir*, 2019, **35**, 11503–11511.

16 H. Xiao, B. Liu, L. Qiu, G. Li, G. Zhang, D. Huang, Y. Zhao, C. Yang, F. Jiang, P. Dang, H. Lian, Z. Cheng and J. Lin, *Angew. Chem., Int. Ed.*, 2022, **61**, e202115136.

17 W. Huang, M. Xu, J. Liu, J. Wang, Y. Zhu, J. Liu, H. Rong and J. Zhang, *Adv. Funct. Mater.*, 2019, **29**, 1808762.

18 X. Kang, Y. Li, M. Zhu and R. Jin, *Chem. Soc. Rev.*, 2020, **49**, 6443–6514.

19 Y. Wu, M. R. K. Ali, K. Chen, N. Fang and M. A. El-Sayed, *Nano Today*, 2019, **24**, 120–140.

20 I. Chakraborty and T. Pradeep, *Chem. Rev.*, 2017, **117**, 8208–8271.

21 X. Ran, Z. Wang, F. Pu, E. Ju, J. Ren and X. Qu, *Mater. Horiz.*, 2021, **8**, 1769–1775.

22 Y. Zheng, J. Wu, H. Jiang and X. Wang, *Coord. Chem. Rev.*, 2020, **431**, 213689.

23 J. Zhang, L. Mou and X. Jiang, *Chem. Sci.*, 2020, **11**, 923–936.

24 H. Zhang, Y. Cao, D. Xu, N. S. Goh, G. S. Demirer, S. Cestellos-Blanco, Y. Chen, M. P. Landry and P. Yang, *Nano Lett.*, 2021, **21**, 5859–5866.

25 J. Shen, Q. Xiao, P. Sun, J. Feng, X. Xin, Y. Yu and W. Qi, *ACS Nano*, 2021, **15**, 4947–4955.

26 N. Xia and Z. Wu, *Chem. Sci.*, 2021, **12**, 2368–2380.

27 J. V. Rival, P. Mymoona, R. Vinoth, A. M. V. Mohan and E. S. Shibu, *ACS Appl. Mater. Interfaces*, 2021, **13**, 10583–10593.

28 X. Kang and M. Zhu, *Chem. Soc. Rev.*, 2019, **48**, 2422–2457.

29 Z. Yu, B. Musnier, K. D. Wegner, M. Henry, B. Chovelon, A. Desroches-Castan, A. Fertin, U. Resch-Genger, S. Bailly, J.-L. Coll, Y. Usson, V. Josserand and X. Le Guével, *ACS Nano*, 2020, **14**, 4973–4981.

30 X. Song, W. Zhu, X. Ge, R. Li, S. Li, X. Chen, J. Song, J. Xie, X. Chen and H. Yang, *Angew. Chem., Int. Ed.*, 2021, **60**, 1306–1312.

31 Z. Pang, Q. Li, Y. Jia, W. Yan, J. Qi, Y. Guo, F. Hu, D. Zhou and X. Jiang, *Chem. Sci.*, 2021, **12**, 14871–14882.

32 C. Yi, Y. Yang, B. Liu, J. He and Z. Nie, *Chem. Soc. Rev.*, 2020, **49**, 465–508.

33 W. Zhang, H. Kong, Z. Wu, Q. Yao, L. Wang, L. Qiao, Y. He, X. Qiao, X. Pang and J. Xie, *Chem. Mater.*, 2021, **33**, 5067–5075.

34 J. Hu, T. Wu, G. Zhang and S. Liu, *J. Am. Chem. Soc.*, 2012, **134**, 7624–7627.

35 T. Zhou, J. Zhu, L. Gong, L. Nong and J. Liu, *J. Am. Chem. Soc.*, 2019, **141**, 2852–2856.

36 T. Zhou, Q. Li, Y. Chen and X. Jiang, *Chem. Commun.*, 2020, **56**, 14023–14026.

37 M. Fukao, A. Sugawara, A. Shimojima, W. Fan, M. A. Arunagirinathan, M. Tsapatsis and T. Okubo, *J. Am. Chem. Soc.*, 2009, **131**, 16344–16345.

38 J. Dey, S. Kumar, S. Nath, R. Ganguly, V. K. Aswal and K. Ismail, *J. Colloid Interface Sci.*, 2014, **415**, 95–102.

39 S. Bonacchi, S. Antonello, T. Dainese and F. Maran, *Chem. - Eur. J.*, 2021, **27**, 30–38.

40 Z. Dai, Y. Tan, K. He, H. Chen and J. Liu, *J. Am. Chem. Soc.*, 2020, **142**, 14023–14027.

41 C. Zhou, C. Sun, M. Yu, Y. Qin, J. Wang, M. Kim and J. Zheng, *J. Phys. Chem. C*, 2010, **114**, 7727–7732.

42 R. J. Banga, B. Meckes, S. P. Narayan, A. J. Sprangers, S. T. Nguyen and C. A. Mirkin, *J. Am. Chem. Soc.*, 2017, **139**, 4278–4281.

43 S. Zanarini, E. Rampazzo, S. Bonacchi, R. Juris, M. Marcaccio, M. Montalti, F. Paolucci and L. Prodi, *J. Am. Chem. Soc.*, 2009, **131**, 14208–14209.

44 H. L. Ma, T. Y. Zhou, Z. Y. Dai, J. Q. Hu and J. B. Liu, *Adv. Opt. Mater.*, 2019, **7**, 1900326.

45 D. Wang and T. P. Russell, *Macromolecules*, 2018, **51**, 3–24.

46 R. Nagarajan, *Colloids Surf., B*, 1999, **16**, 55–72.

47 M. Zhou and Y. Song, *J. Phys. Chem. Lett.*, 2021, **12**, 1514–1519.

48 Z. Zhang and Y. Wu, *Langmuir*, 2010, **26**, 9214–9223.

49 **https://www.computerhope.com/jargon/a/ascii.htm#convert**.